Tension Lines of the Skin

Aisling Ní Annaidh and Michel Destrade

Abstract Skin tension lines are natural lines of tension that occur within the skin as a result of growth and remodeling mechanisms. Researchers have been aware of their existence and their surgical implications for over 150 years. Research in the twentieth century showed clearly, through destructive mechanical testing, that the orientation of skin tension lines greatly affects the mechanical response of skin in situ. More recent work has determined that this anisotropic response is, at least in part, due to the structural arrangement of collagen fibres within the dermis. This observation can be incorporated into mathematical and mechanical models using the popular Gasser-Ogden-Holzapfel constitutive equation. Advances in non-invasive measurement techniques for the skin, such as those based on elastic wave propagation, have enabled patient-specific identification of skin tension lines in an accurate and rapid manner. Using this technique on humans, we show that there is considerable variation in the level of anisotropy as the skin ages. Furthermore, we identify that both the structural arrangement of fibres and the in vivo levels of pre-strain play a significant role in the anisotropic behavior of skin.

A. Ní Annaidh
School of Mechanical & Materials Engineering, University College Dublin, Dublin 4, Ireland

UCD Charles Institute of Dermatology, School of Medicine and Medical Science, University College Dublin, Dublin, Ireland
e-mail: aisling.niannaidh@ucd.ie

M. Destrade (✉)
Stokes Centre for Applied Mathematics, School of Mathematics, Statistics and Applied Mathematics, NUI Galway, Galway, Ireland

School of Mechanical & Materials Engineering, University College Dublin, Dublin 4, Ireland
e-mail: michel.destrade@nuigalway.ie

1 Historical Beginnings and Clinical Significance

As is the case for most biological soft tissues, an inherent residual stress exists in the skin [1–3]. It is due to growth and remodelling mechanisms [4] and is, in general, very complex to model and evaluate [5]. In human skin, the presence of residual stress has important implications for surgical planning and forensic science, as it can affect significantly the extent of gaping following a cut, and then the resulting healing time. The so-called *Langer Lines* are often considered to be the lines of maximum in vivo tension in the skin. They form an involved map over the body. To minimise the likelihood of excessive wound tension, wound rupture and subsequent unsightly scars, surgical incisions should be made parallel to Langer lines, which lie along the path of maximum skin tension [6].

The discovery of tension lines in skin is widely attributed to a nineteenth Century Austrian surgeon, Karl Langer, after whom the lines are named. The conventional wisdom is that Langer identified the existence of skin tension lines in 1861. In fact, Guillaume Dupuytren, a French anatomist and military surgeon, had made this observation earlier, as early as 1834. Langer's contribution was to systematically puncture the skin of cadavers with multiple circular wounds and indicate the major axes of the resulting ellipses [7]. When viewed together, these ellipses form a map of the natural lines of skin tension, see Fig. 1. Kocher explicitly linked the direction of Langer lines, or cleavage lines, to recommended orientations for surgical incisions and observed that incisions made along these lines will cause little or no scarring, whereas incisions transverse to them will gape and result in unsightly scars [9].

While Langer lines are the best known skin tension lines, many variations on the original lines proposed by Langer have been made over the years. In 1951, for example, Kraissl [10] suggested that surgeons should incise along natural wrinkle lines rather than along the Langer lines. In 1984, Borges [6] defined the Relaxed
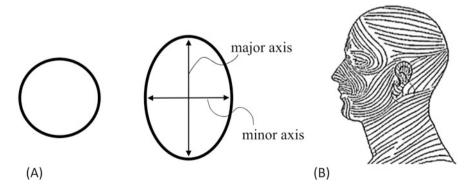

Fig. 1 (**a**) Original circular wound geometry and deformed ellipsoidal wound geometry due to skin tension (**b**) Langer Lines of the face created by joining the major axis of each deformed wound. Reproduced from [8]

Skin Tension Lines (RSTL). These lines follow furrows when the skin is relaxed and can be identified visually by pinching the skin. In his historical account, Carmichael [11] identified a non-exhaustive list of no less than 46 different types of skin lines, folds and planes of the skin recorded in the literature from 1861 [7] to 2004 [12]. Most of these lines have similarities with the original Langer Lines in that they are related to the natural lines of skin tension and seek to assist in surgical planning to ensure the best outcomes in terms of the aesthetics of the resulting scar. To avoid confusion, for the remainder of this chapter, we will use the term "skin tension lines" (STL) to refer to the orientation of maximum skin tension.

Until recently, the orientation of the STLs could not be identified with certainty unless the skin was punctured by a circular punch, an option which is generally neither feasible nor practical. In the first part of this chapter, we show how destructive, invasive techniques have been used to determine the orientation of the STLs and to develop a fundamental understanding of the skin's structure. By now, it is well accepted that the STLs vary with location on the body, age, ethnicity, body mass index, health, gender, etc., and that no fully universal pattern of maximum tensions exists [13]. Given the importance of STLs on the mechanical properties of skin and wound closure, there is a pressing need for patient-specific maps to be established in vivo and in real time. In this respect, recent advances in elastic wave propagation techniques have facilitated non-invasive, in vivo identification of skin tension lines [14, 15]. In the second part of this chapter, we show that a simple device, based on elastic wave propagation, can perform these tasks without damaging the skin.

2 Invasive Investigation of the Skin Tension Lines

2.1 *Mechanical Behaviour with Respect to Skin Tension Lines*

Early tensile tests suggested that the deformation characteristics of skin are dependent on specimen orientation with respect to the STLs. Ridge et al. [16] carried out uniaxial tensile tests on human cadavers both parallel and perpendicular to the STLs and found that the samples parallel to the STLs had higher stiffness, as shown in Fig. 2a. On the basis of this observation, an idealised collagen fibre mesh structure was proposed, as shown in Fig. 2b. The fibres were assumed to form an interweaving lattice structure with a mean angle less than 45°. Later, Lanir and Fung [17] performed biaxial tests on skin samples taken from the abdomen of rabbits, confirming that skin is strongly anisotropic and probably possessing orthotropic symmetry. It was also reported that during stress-relaxation tests there were considerable alterations to the transverse dimensions, indicating that relaxation behaviour may also be orthotropic. On the basis of these findings, researchers now
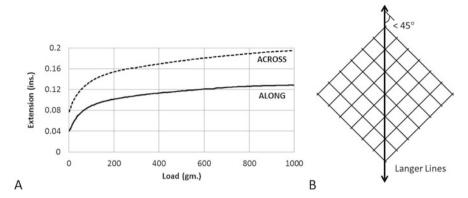
Fig. 2 (**a**) Load-extension curve along and across the Langer lines. (**b**) The proposed lattice structure of collagen fibres. Reproduced from [16]

commonly use the plane containing the STLs as a reference plane, as opposed to e.g., the sagittal plane.

While uniaxial tensile tests alone are not sufficient to determine multi-dimensional material models for soft tissues, they remain important because they serve to evaluate the level of anisotropy and provide data which can later be used as validation for models constructed using more complicated testing methods [18]. Moreover, constitutive model parameters can be determined directly from a histological study of the collagen fibre alignment in the dermis, which allows for reasonable determination of material responses [19].

In [20] human skin was excised from the backs of seven human subjects: three male, four female, with the average age of the subjects being 89 ± 6 years. A total of 56 specimens were excised in various orientations with respect to the perceived orientation of STLs, shown in Fig. 3a, and each sample was grouped into one of three categories: parallel, perpendicular, or at 45° to the STLs. Uniaxial tensile tests were performed at a strain rate of 0.012/s. A number of characteristics from nominal stress vs. stretch ratio curves were identified as descriptive parameters. They are illustrated in Fig. 3b.

A multiway analysis of variance found the orientation of STLs to have a significant effect on the ultimate tensile strength ($P < 0.0001$), the strain energy ($P = 0.0101$), the elastic modulus ($P = 0.0002$), the initial slope ($P = 0.0375$), and the failure stretch ($P = 0.046$). The interaction between orientation and location was also tested i.e., whether the effect of orientation was dependent upon location. This interaction between orientation and location was found to be significant only for the failure stretch ($P = 0.0118$). These results are illustrated in Fig. 4 and reproduced in Table 1. From these experimental studies, it is clear that the mechanical behaviour of skin varies with respect to the STLs.
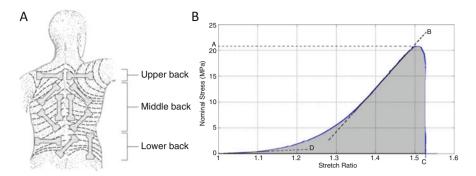
Fig. 3 (**a**) Orientation of samples from the back with respect to the STLs [7]. (**b**) Typical stress-stretch graph for uniaxial tension experiments. The ultimate tensile strength is the maximum stress until failure of the specimen and is indicated by A. The elastic modulus is defined as the slope of the linear portion of the curve shown by B. The failure stretch is the maximum stretch obtained before failure and is shown by C. The initial slope is the slope of the curve at infinitesimal strains and is shown by D. The strain energy is the energy per unit volume consumed by the material during the experiment and is represented by the area under the curve [20]
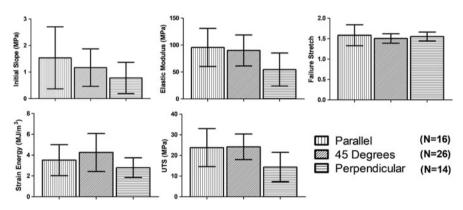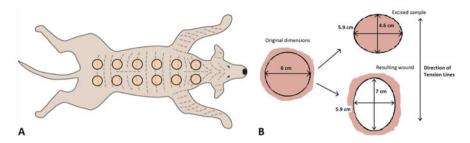

Fig. 4 Influence of orientation on the initial slope, elastic modulus, failure stretch, strain energy and ultimate tensile strength (UTS). Values given include mean and standard deviation [20]

2.2 Shrinkage and Expansion with Respect to Skin Tension Lines

It is known that both shrinkage and expansion of specimens can occur upon excision from the body [16, 17, 21, 22]. This is due to the release of residual stresses within the skin. What remains unclear is the level of residual stress present within the skin and how this may vary with the orientation of specimens. Upon excision of skin samples from the body, Ridge and Wright [16] observed that the greatest shrinkage occurred in the direction of Langer lines, with a shrinkage of 9% parallel to the Langer lines and 5% perpendicular to the Langer lines. They also observed a

Table 1 Summary of uniaxial tensile test results on human skin with respect to sample orientation and location (mean ± standard deviation for each orientation/location group) [20]

STL orientation	Location	N	UTS (MPa)	Strain energy (MJ/m^3)	Failure stretch	Elastic modulus (MPa)	Initial slope (MPa)
Parallel	Middle	9	28.64 ± 9.03	4.28 ± 1.49	1.46 ± 0.07	112.47 ± 36.49	1.21 ± 0.97
Parallel	Bottom	7	17.60 ± 4.77	2.54 ± 0.76	1.74 ± 0.32	73.81 ± 19.41	1.95 ± 1.34
45°	Top	12	22.7 ± 3.61	3.80 ± 0.92	1.52 ± 0.10	82.62 ± 17.36	0.99 ± 0.51
45°	Middle	9	28.85 ± 7.87	5.38 ± 2.59	1.52 ± 0.15	103.49 ± 41.20	1.33 ± 0.96
45°	Bottom	5	20.23 ± 4.18	3.31 ± 0.67	1.43 ± 0.04	82.81 ± 18.43	1.30 ± 0.60
Perpendicular	Middle	9	16.53 ± 5.71	2.98 ± 0.89	1.52 ± 0.08	63.75 ± 24.59	0.91 ± 0.68
Perpendicular	Bottom	5	10.56 ± 8.41	2.44 ± 1.04	1.61 ± 0.14	37.66 ± 36.41	0.54 ± 0.33

Fig. 5 (**a**) Sample locations of circular samples removed from dog cadaver (**b**) Illustration of average contraction and expansion levels with respect to the skin tension lines for (1) an isolated excised sample (2) an originally excise wound [14]

large difference in the level of shrinkage between males and females. Reihmer and Menzel [23] carried out multiaxial tension tests using a customised device, where excised circular samples were radially stretched by a ring of pullers placed at 30° intervals around the circumference, restoring the in vivo shape of the excision. They confirmed that the axes of minimum and maximum shrinkage after excision were correlated with the orientation of STLs and that the in vivo were determined by restoring the original shape of the specimen.

More recently, Deroy et al. [14], using a dog cadaver model, showed that the average area expansion of the circular wounds was 9%, corresponding to a line expansion of 16% parallel to the STLs (by image analysis), but a line contraction of 10% perpendicular to the STLs. Similarly, the area of the excised sample shrank by 33% overall, shrinking 23% parallel to the STLs and shrinking 10% perpendicular to the STLs. Figure 5 provides a summary of the levels of expansion and contraction of both the excised skin sample and the resulting wound.

2.3   Structural Basis of Skin Tension Lines

Cox [21] and Stark [24] both illustrated that the orientations of STLs are preserved even after the skin is removed from the body and the skin tension released, and concluded that the lines must have an anatomical basis. However until the publication of papers by Ní Annaidh et al. [25] and Deroy et al. [14], it was unclear in the literature whether the STLs had a structural basis, and to the authors' knowledge there was no previous quantitative data published on this point. Van Zuijlen et al. [26] and Noorlander et al. [27] used Fourier analysis to measure the level of anisotropy of collagen in the skin but failed to provide information on the mean orientation of the fibres. While in Jor et al. [28], histology techniques provided quantitative results on the orientation of collagen fibres in porcine skin, but results were presented in the plane normal to the epidermis/skin surface (i.e.

through-the-thickness direction) while the preferred orientation of collagen fibres in skin is known to be parallel to the epidermis surface [5, 25].

It is well known that collagen fibres govern many of the mechanical properties of soft tissues, in particular their anisotropic behaviour (at least partly, as strain-induced anisotropy can also play a role, as we will see later.) A number of authors have sought to incorporate their influence in constitutive models of soft tissues. Gasser at al. [29] developed a now widely accepted structural model for arterial layers which includes a parameter representing the dispersion of collagen fibres. The inclusion of the collagen dispersion factor is particularly useful for application to human skin, since the orientations of collagen fibres there are more dispersed than say in the tendon or media layer of the artery [25]. The corresponding Gasser-Ogden-Holzapfel (GOH) strain energy function, Ψ, is given by

$$\Psi = \frac{\mu}{2}(I_1 - 3) + \mu\frac{k_1}{k_2}\left\{e^{k_2[\kappa I_1 + (1-3\kappa)I_4 - 1]^2} - 1\right\}$$

where μ, k_1 and k_2 are positive material constants, κ is the dispersion factor, and I_1 and I_4 are strain invariants, with I_1 related to the isotropic behaviour of the tissue matrix and I_4 related to the anisotropic behaviour due to the fibre contribution.

Using automated image processing of histological skin sections summarised in Fig. 6, Ní Annaidh et al. [25] determined the quantitative structural parameters of the GOH model for the human dermis. Two distinct peaks are evident from Fig. 6c. It is assumed that these two peaks correspond to the preferred orientation of two crossing families of fibres and are distributed according to a π-periodic von Mises distribution. The standard π-periodic von Mises distribution is normalized and the resulting density function, $\rho(\theta)$, reads as follows,

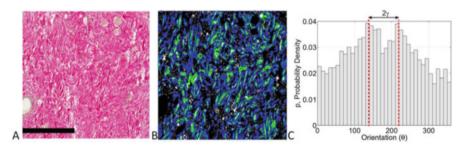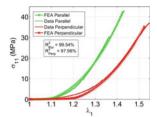$$\rho(\theta) = 4\sqrt{\frac{b}{2\pi}}\frac{\exp[b(\cos(2\theta)) + 1]}{erfi(\sqrt{2b})}$$

Fig. 6 (**a**) Original histology slide sectioned parallel to the epidermis and stained with Van Gieson to highlight collagen fibres as pink. Scale bar is 1 mm. (**b**) After morphlical operations, the predominant orientations of fibres bundles are identified by determining the orientation of best fit ellipses. (**c**) The predominant orientations of fibre bundles are plotted on a histogram and fit to a π-periodic Von Mises distribution

Fig. 7 FEA simulation of tensile test compared with experimental data of sample parallel and perpendicular to the STLs. Material parameters used in the simulation. Note that structural parameters (γ, θ, κ) were evaluated from histological data [25]

where b is the concentration parameter associated with the von Mises distribution and θ is the mean orientation of fibres. The parameters b and θ were evaluated using maximum likelihood estimates (MLE) and κ was calculated by numerical integration of the integral given by [29],

$$\kappa = \frac{1}{4}\int_0^\pi \rho\left(\theta\right) sin^3\theta d\theta$$

The fibres were assumed to form an interweaving lattice structure as first postulated by Ridge and Wright [30]. Those authors suggested that the mean angle of the two families of fibres indicates the direction of the Langer lines. More recently, in vitro [28] and in vivo [31] studies have also supported this hypothesis. The lattice structure proposed by Ridge and Wright [30] is an idealised one, and the adoption here of the dispersion factor creates a more realistic scenario. Using the identified structural constitutive parameters for both a sample parallel and perpendicular to the STLs, Fig. 7 illustrates the potential of the GOH model to predict the mechanical behaviour of a sample, given known structural parameters.

3   Noninvasive Investigation of the Skin Tension Lines

In this second part of the chapter, we will see how the orientation of STLs can be determined accurately, locally, rapidly, non-destructively, and non-invasively. This possibility is highly desirable for planned surgery, because STLs are known to be patient-specific and can depend on a multitude of factors, including location, age, health, body mass index, ethnicity, hydration, gender, corpulence, etc., and of course, differ from one species to another. Minimizing scalpel cutting force, wound healing time, and scar tissue extent are goals of prime importance to surgeons and patients alike. Here we show how a small acoustic device can determine the directions of STLs, based on some simple principles and on logic.

We use the Reviscometer® RVM600 (Courage & Khazaka Electronic GmbH, Köln, Germany), a commercial device aimed primarily at the cosmetic and derma-

tology industry [31–33], and based on a simple operating principle. Basically it is a probe consisting of two small indenters, 2 mm apart, coming into contact with the skin. One hits the skin with a force of 1 N, and the other receives the resulting mechanical signal generated and travelling in the skin. The machine returns the time it took to travel the 2 mm distance, the so-called RRT ("resonance running time"), although this measurement is provided in arbitrary units and its relationship with standard units, i.e. seconds, is not provided by the manufacturer. The probe can then be rotated by 10° increments, to give the variations of the RRT with angle. With this information, we can actually address the following questions, using experimental observations and logic:

- Is the skin anisotropic?
- How many directions of preferred orientation does it possess?
- Do the mechanical properties of skin change with age?
- What is the orientation of the STLs at a given location?
- Is the anisotropy due to stretch alone, to fibres alone, or a combination?
- How many families of parallel fibres are there?

First, we conduct a series of 36 measurements on the lower volar forearm area of a 21 year old human female. Figure 8 shows the apparatus and displays the results given by the measurements, averaged over the 36 series.

This simple experiment clearly shows that *skin is anisotropic*. On inspection, we see that the results reveal *two preferred directions*: one where the acoustical signal generated by the probe travels at its fastest in the skin (blue minima at 60° and at $60 + 180 = 240°$) and another where it travels at its slowest (green maxima at 150° and 330°). Those *two directions are at right angle* to one another.

Next we may use the Reviscometer® to investigate the *influence of age and gender on the mechanical properties of skin*. The measured values of the RRT are not useful from the point of view of physics, because it proves difficult to calibrate the Reviscometer against an engineering material with known properties. Nonetheless, we can use the ratio $A = RRT_{max}/RRT_{min}$ of its highest to its smallest value as a dimensionless measure of the skin anisotropy, and track if and how it
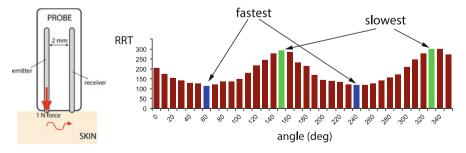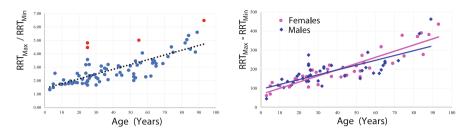

Fig. 8 The Reviscometer applied on skin in the lower volvar forearm area. Its measurements clearly show two directions at right angle one to the other, where the acoustic signal travels at its fastest and at its slowest

Table 2 Age distribution of the cohort of 78 volunteers tested on their volar forearm skin

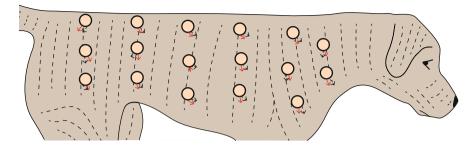| Age (years)	0–10	10–20	20–30	30–40	40–50	50–60	60–70	70+
Sample size	7	10	16	11	7	10	7	10

Fig. 9 (left) Variation of the anisotropic index RRT_{max}/RRT_{min} with age for the skin on the volar forearm skin of 78 volunteers. (right) Variation of the anisotropic range RRT_{max}-RRT_{min} with age, with gender distinction (circles: females, squares: males)

evolves with age and gender. To this end, we tested a total of 78 volunteers (37 female, 41 male), aged 3–93 years of age, see Table 2. We conducted the tests at University College Dublin, having secured ethical approval (LS-15-65-NiAnnaidh).

We found a significant linear relationship between the Anisotropic Index, *A* (where the Anisotropic Index refers to the ratio of the maximum RRT: minimum RRT about a full 360° for a given site) and age (P < 0.0005), as shown in Fig. 9. An R^2 value of 0.59 indicates that age accounted for a significant amount of the explained variability in the Anisotropic Index, but it suggests that the linear model is merely adequate. There were a number of unusual observations with large standardised residual values, as some outliers (in red) do not fit the model. We noted that these outliers belong to Asian ethnic groups while the remainder of the cohort were Caucasian Irish, but we did not have enough volunteers to account for this factor. When we accounted for gender, we did not find significant differences for the data on the volar forearm skin.

So far, we have seen that the Reviscometer® indicates two distinct orthogonal on in vivo skin, but how are these directions of fast and slow mechanical wave propagation related to the Skin Tension Lines? To address that question, we simply compare those directions to those resulting from the original protocol devised by Langer.

For these experiments, we used the skin of dog cadavers. Although designed to work optimally on human skin, the Reviscometer® also works well on dog skin, even though dog skin is known to be stiffer and somewhat thicker than human skin [14, 20]. We performed the testing at the University College Dublin School of Veterinary Medicine on the cadavers of two healthy young adult dogs. First, we drew circles on the skin of one dog, and used the Reviscometer® to determine the direction of fastest wave at each location. Then we excised 6 mm circular discs from the skin at those locations and watched them change shape due to the in situ skin tension. Using image analysis, we fitted the wounds to ellipses and determined the

Fig. 10 Comparing the local lines of fastest mechanical wave propagation given by the Reviscometer (black arrows) to the orientation of the Skin Tension Lines (red arrows) as determined by Langer's original protocol of cutting a circular hole out of the skin and recording the direction of the major axis in the resulting elliptical shape. The experiments were conducted on a 5-year-old female, mixed-breed, medium sized dog cadaver at University College Dublin

orientation of their major axis. We found a significant statistical correlation between the orientation of the major axes of the resulting elliptical wounds and the direction of fastest wave propagation. In other words, the Reviscometer® device provides *a non-invasive, non-destructive way of determining the STLs locally*. Of course, this study is limited in its scope and the experimental uncertainty is still an issue, but these limitations can be addressed with further and wider trials. The results of the two techniques are compared directly in Fig. 10.

At this stage, we can contemplate several scenarios to explain the anisotropy of the RRT response. It could be due to

  i. Fibres only;
 ii. Strain only;
iii. A combination of both.

We can safely exclude (i) straightaway, because it is obvious that skin is stretched in the body, as shown by our and Langer's experiments, and as attested by anyone who has cut themselves and seen their wound gape open. On the other hand, deciding between the second and third possibility is not so obvious.

Resorting now to *modelling*, we can make the reasonable assumption that the probe is sensitive to vertical displacements only, based on its working principle. To model these vertical motions, we focus on homogeneous, linearly polarised plane waves, for which the components of the mechanical displacement $\boldsymbol{u}$ are of the form

$$u_1 = 0, u_2 = 0, u_3 = ae^{ik(\boldsymbol{n}.\boldsymbol{x}-vt)},$$

where a is the amplitude, k is the wavenumber, $\boldsymbol{n} = \cos\theta\,\boldsymbol{i} + \sin\theta\,\boldsymbol{j}$ is the unit vector in the direction of propagation, and v is the wave speed. Here we took the skin to be normal to the x_3-axis, and the x_1, x_2 axes to be aligned with the principal axes of strain. We assume that the fibres, if they exist, are lying in the (x_1, x_2) plane. Because the surface of the skin in the upper arm volar area and on the
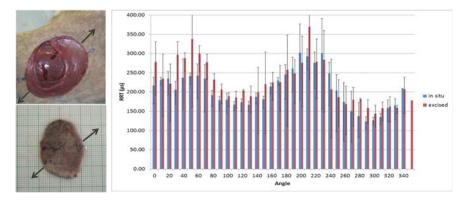
chosen locations in the dog cadaver is flat and smooth, we can also assume that it is deformed homogeneously and not subject to shear forces, which would create wrinkles at rest [34]. It follows that if there is only one family of parallel fibres, then they must be aligned with one of the principal directions of strain. If there are two families of parallel fibres, then they must either be at right angle and aligned with the principal axes, or be mechanically equivalent with their bisectors aligned with the principal axes [25]. Whether the anisotropy is due to strain only or to a mixture of strain and fibres (Cases ii and iii above), the wave speed is given by the same formula, as follows,

$$\rho v^2 = \mathcal{A}_{01313}(\cos\theta)^2 + \mathcal{A}_{02323}(\sin\theta)^2,$$

where ρ is the mass density and the $\mathcal{A}_0$'s are the instantaneous shear moduli, computed from the second derivatives of the strain energy density with respect to the strain [35]. In either case—whether fibres are present or not—the variation of RRT with angle resulting from the equation above is compatible with the RRT profiles found, see Fig. 8.

To settle the question, we rely on the Reviscometer® again. On the skin of the second dog cadaver, we repeated the procedure of identifying the Langer Lines by determining the fastest wave direction and matching it to the principal minor axis of the resulting elliptical wound. This time, however, we cut out larger discs (6 cm diameter). Then, on those ex-vivo discs, which were completely free of initial stress and had turned into ellipses, we *again* made measurements with the Reviscometer® device. The results were again anisotropic, see Fig. 11, and this observation can only be attributed to the presence of oriented fibres.

The other insight that came out of the latter experiments was that we found the directions of anisotropy for the unstressed discs to be the same as those noted

Fig. 11 RRT measurements before (red) and after (blue) excision of a 6 cm disc. The excised sample displays anisotropy and thus demonstrates the presence of fibres in the skin. Both samples indicate the same direction of fastest wave, and thus show that fibres are aligned with Langer lines in situ

when in situ. This observation is proof that *in the body, fibres are aligned with the principal axes of strain.* Hence we can exclude the possibility of anisotropy due to two families of parallel fibres, mechanically equivalent, with their bisectors aligned with the principal axes of strain. We also recorded that the amplitude of the RRT anisotropy was noticeably reduced once the discs had been removed, while the RRT itself had increased, confirming that in vivo tension plays a significant mechanical role in the skin, of the same order as the contribution from the fibres. The only question that our investigation could not address was whether there was one or two families of parallel fibres aligned with the principal axes of strain. Here we must rely on the indications given by the destructive testing described in the first part of the chapter, which tell us that there are indeed two families of parallel fibres in the skin. Making the reasonable assumption that the fibres orthogonal to the directions of tension are contracted, we can ignore their mechanical contribution and conclude that in the body at rest, *active fibres are aligned with the Langer Lines.*

4 Conclusion

Assessing the body of literature examining *destructive* testing of skin, we have confirmed that its mechanical properties, in particular the stiffness and the level of shrinkage once excised from the body, depend heavily on their orientation with respect to skin tension lines. Histological investigations have supported the hypothesis that the STLs have a structural basis, while recent *non-invasive* testing of skin has shed further light on this matter. It is now clear that in the body, fibres are aligned with the principal axes of strain and that both the alignment of collagen fibres and the in vivo strain play a significant role in the mechanical response of the skin. Since it is non-invasive, in vivo evaluation techniques such as elastic wave propagation offer significant potential in the investigation of the ageing of skin and in the patient specific planning of surgical procedures. Further research should seek to develop models to accurately reflect the mechanical environment.

References

1. Alexander H, Cook TH (1977) Accounting for natural tension in the mechanical testing of human skin. J Invest Dermatol 69(3):310–314
2. Holzapfel GA (2005) Similarities between soft biological tissues and rubberlike materials. In: Austrell P-E, Kari L (eds) Constitutive models for Rubber IV. Taylor & Francis, London, pp 607–618
3. Flynn C, McCormack BAO (2010) Simulating the wrinkling and aging of skin with a multi-layer finite element model. J Biomech 43(3):442–448
4. Rodriguez EK, Hoger A, McCulloh AD (1994) Stress dependent finite growth in soft elastic tissues. J Biomech 27:455–467

5. Holzapfel GA (2001) Biomechanics of soft tissue. In: Lemaitre J (ed) Handbook of materials behavior models. Academic Press, Burlington, pp 1057–1071
6. Borges AF (1984) Relaxed Skin Tension Lines (RSTL) versus other skin lines. Plast Reconstr Surg 73(1):144–150
7. Langer K (1861) On the anatomy and physiology of the skin. The Imperial Academy of Science, Vienna. Reprinted in (1978). Br J Plast Surg 17(31):93–106
8. Fagan J (2014) Open Access Atlas of Otolaryngology, Head & Neck Operative Surgery. Cape Town University. http://doer.col.org/handle/123456789/6513
9. Kocher T (1892) Chirurgische operationslehre. G. Fischer, Jena
10. Kraissl CJ (1951) The selection of appropriate lines for elective surgical incisions. Plast Reconstr Surg 8(1):1–28
11. Carmichael SW (2014) The tangles web of langer's lines. Clin Anat 27:162–168
12. Sarıfakıoğlu N et al (2004) A new phenomenon: "sleep lines" on the face. Scand J Plast Reconstr Surg Hand Surg 38(4):244–247
13. Brown IA (1973) A scanning electron microscope study of the effects of uniaxial tension on human skin. Br J Dermatol 89:383–393
14. Deroy C et al (2017) Non-invasive evaluation of skin tension lines with elastic waves. Skin Res Technol 23(3):326–335
15. Liang X, Boppart SA (2010) Biomechanical properties of in vivo human skin from dynamic optical coherence elastography. IEEE Trans Biomed Eng 57(4):953–959
16. Ridge MD, Wright V (1966) The directional effects of skin. A bio-engineering study of skin with particular reference to Langer's lines. J Invest Dermatol 46(4):341–346
17. Lanir Y, Fung YC (1974) Two-dimensional mechanical properties of rabbit skin. II. Experimental results. J Biomech 7(2):171–174
18. Holzapfel GA, Ogden RW (2009) On planar biaxial tests for anisotropic nonlinearly elastic solids. A continuum mechanical framework. Math Mech Solids 14(5):474–489
19. Holzapfel GA (2006) Determination of material models for arterial walls from uniaxial extension tests and histological structure. J Theor Biol 238(2):290–302
20. Ní Annaidh A et al (2012) Characterising the anisotropic mechanical properties of excised human skin. J Mech Behav Biomed Mater 5:139–148
21. Cox HT (1941) The cleavage lines of the skin. Br J Surg 29(114):234–240
22. Jansen LH, Rottier PB (1958) Some mechanical properties of human abdominal skin measured on excised strips. Dermatologica 117:65–83
23. Reihsner R, Menzel EJ (1996) On the orthogonal anisotropy of human skin as a function of anatomical region. Connect Tissue Res 34(2):145–160
24. Stark HL (1977) Directional variations in the extensibility of human skin. Br J Plast Surg 30(2):105–114
25. Ni Annaidh A et al (2012) Automated estimation of collagen fibre dispersion in the dermis and its contribution to the anisotropic behaviour of skin. Ann Biomed Eng 40(8):1666–1678
26. Van Zuijlen PPM et al (2002) Morphometry of dermal collagen orientation by Fourier analysis is superior to multi-observer assessment. J Pathol 198:284–291
27. Noorlander ML et al (2002) A quantitative method to determine the orientation of collagen fibers in the dermis. J Histochem Cytochem 50(11):1469–1474
28. Jor JWY et al (2011) Modelling collagen fibre orientation in porcine skin based upon confocal laser scanning microscopy. Skin Res Technol 17(2):149–159
29. Gasser T, Ogden RW, Holzapfel G (2006) Hyperelastic modelling of arterial layers with distributed collagen fibre orientations. J R Soc Interface 3:15–35
30. Ridge MD, Wright V (1966) Mechanical properties of skin: a bioengineering study of skin structure. J Appl Physiol 21:1602–1606
31. Ruvolo JEC, Stamatas GN, Kollias N (2007) Skin viscoelasticity displays site- and age-dependent angular anisotropy. Skin Pharmacol Physiol 20:313–321
32. Paye M et al (2007) Use of the Reviscometer for measuring cosmetics-induced skin surface effects. Skin Res Technol 13:343–349

33. Quatresooz P et al (2008) Laddering melanotic pattern of Langer's lines in skin of colour. Eur J Dermatol 5:575–578
34. Ciarletta P, Destrade M, Gower AL (2013) Shear instability in skin tissue. Q J Mech Appl Math 66(2):273–288
35. Destrade M (2015) Incremental equations for soft fibrous materials. In: Dorfmann L, Ogden RW (eds) Nonlinear mechanics of soft fibrous materials. Springer, Vienna, pp 233–267